Received: 12 January 2017 | Revised: 22 September 2017 | Accepted: 23 September 2017

DOI: 10.1111/pce.13084

WILEY Plant, Cell & Environment

ORIGINAL ARTICLE

The genetic architecture of photosynthesis and plant growth-related traits in tomato

Franklin Magnum de Oliveira Silva[1] | Gabriel Lichtenstein[2] | Saleh Alseekh[3] | Laise Rosado-Souza[3] | Mariana Conte[2] | Vanessa Fuentes Suguiyama[4] | Bruno Silvestre Lira[5] | Dimitrios Fanourakis[6] | Björn Usadel[7,8] | Leonardo Lopes Bhering[9] | Fábio M. DaMatta[10] | Ronan Sulpice[11] | Wagner L. Araújo[1] | Magdalena Rossi[5] | Nathalia de Setta[4] | Alisdair R. Fernie[3] | Fernando Carrari[2] | Adriano Nunes-Nesi[1]

[1] Max-Planck Partner Group, Departamento de Biologia Vegetal, Universidade Federal de Viçosa, 36570-900 Viçosa, Minas Gerais, Brazil

[2] Instituto de Biotecnología, Instituto Nacional de Tecnología Agropecuaría, and Consejo Nacional de Investigaciones Científicas y Técnicas, B1712WAA Castelar, Argentina

[3] Max-Planck-Institute of Molecular Plant Physiology, Am Mühlenberg 1, 14476 Potsdam, Germany

[4] Universidade Federal do ABC, 09606070 São Bernardo do Campo, São Paulo, Brazil

[5] Departamento de Botânica, Instituto de Biociências, Universidade de São Paulo, São Paulo 05508–900, Brazil

[6] Department of Viticulture, Floriculture, Vegetable Crops and Plant Protection, GR 71307 Heraklion, Greece

[7] IBMG: Institute for Biology I, RWTH Aachen University, Worringer Weg 2, 52074 Aachen, Germany

[8] Forschungszentrum Jülich, IBG-2 Plant Sciences, Wilhelm-Johnen-Straße, 52425 Jülich, Germany

[9] Departamento de Biologia Geral, Universidade Federal de Viçosa, 36570-900 Viçosa, Minas Gerais, Brazil

[10] Departamento de Biologia Vegetal, Universidade Federal de Viçosa, 36570-900 Viçosa, Minas Gerais, Brazil

[11] Plant Systems Biology Lab, Plant and AgriBiosciences Research Centre, Plant & Agribiosiences, National University of Ireland Galway, H91 TK33 Galway, Ireland

Correspondence
Adriano Nunes-Nesi, Departamento de Biologia Vegetal, Universidade Federal de Viçosa, 36570-900 Viçosa, Minas Gerais, Brazil.
Email: nunesnesi@ufv.br

Funding information
Conselho Nacional de Desenvolvimento Científico e Tecnológico (CNPq), Grant/Award Number: 306355/2012-4, 401090/2014-0, 484675/2013-3, 401090/2014-0 and 484675/2013-3; Max Planck Society; Fundação de Amparo à Pesquisa do Estado de Minas Gerais (FAPEMIG), Grant/Award Number: APQ-00688-12, APQ-02548-13 and BDS-00040-14

Abstract

To identify genomic regions involved in the regulation of fundamental physiological processes such as photosynthesis and respiration, a population of *Solanum pennellii* introgression lines was analyzed. We determined phenotypes for physiological, metabolic, and growth related traits, including gas exchange and chlorophyll fluorescence parameters. Data analysis allowed the identification of 208 physiological and metabolic quantitative trait loci with 33 of these being associated to smaller intervals of the genomic regions, termed BINs. Eight BINs were identified that were associated with higher assimilation rates than the recurrent parent M82. Two and 10 genomic regions were related to shoot and root dry matter accumulation, respectively. Nine genomic regions were associated with starch levels, whereas 12 BINs were associated with the levels of other metabolites. Additionally, a comprehensive and detailed annotation of the genomic regions spanning these quantitative trait loci allowed us to identify 87 candidate genes that putatively control the investigated traits. We confirmed 8 of these at the level of variance in gene expression. Taken together, our results allowed the identification of candidate genes that most likely regulate photosynthesis, primary metabolism, and plant growth and as such provide new avenues for crop improvement.

KEYWORDS

introgression lines, primary metabolism, quantitative trait loci

1 | INTRODUCTION

Life on earth depends upon the ability of plants to convert solar energy into biomass. Our understanding of the molecular, physiological, and developmental determinants underpinning variation in photosynthesis and related processes, such as respiration and photorespiration, is thus essential for sustaining or even improving plant performance and production. Determination of natural variation in physiological and metabolic processes can uncover key traits associated with plant performance within defined ecological and agricultural settings. As such it can provide insights into the mechanisms involved in adaptation to varying environments, paving the path to predictive models of plant productivity within the context of ongoing global climate change (Mozdzer & Zieman, 2010; Zou, Rogers, & Siemann, 2007). Improvement in photosynthetic efficiency can be achieved via different strategies including improving light capture or light energy conversion, enhancing carbon fixation and carbon conversion, or via bypassing photorespiration (Ort et al., 2015). However, independent elevation of carbon fixation unlinked to an increase in sugar transport and sink strength leads to the accumulation of carbohydrates in leaves resulting in the downregulation of photosynthesis. As a result, strategies to enhance photosynthesis must be placed within the context of whole-plant relationships (Rossi, Bermudez, & Carrari, 2015).

Natural variation in plant photosynthesis exists among and within species (Hikosaka, 2010; Lawson, Kramer, & Raines, 2012) and, therefore, should be explored to identify genetic determinants that may allow further improvement in crop yields (Flood, Harbinson, & Aarts, 2011; Lawson et al., 2012). The genetic variation in chlorophyll *a* fluorescence parameters has been investigated in several species including *Arabidopsis* (El-Lithy et al., 2005; van Rooijen, Aarts, & Harbinson, 2015), wheat (Bertin & Gallais, 2001; Driever, Lawson, Andralojc, Raines, & Parry, 2014; Li et al., 2010; Yang, Jing, Chang, & Li, 2007; Zhang, Fang, Liang, & Tian, 2009), rice (Gu, Yin, Struik, Stomph, & Wang, 2012), and soybean (Yin et al., 2010). Interestingly, screening of *Arabidopsis* accessions using chlorophyll *a* fluorescence as a surrogate for photosynthetic performance indicated that photosynthetic yield is highly stable, suggesting that only severe selective pressure can result in marked variations in photosynthetic performance (El-Lithy et al., 2005). Surprisingly, despite the increasing number of natural variation based studies, the genetic factors involved in the regulation of photosynthesis remain largely unknown (Flood et al., 2011). This is probably because variant alleles are generally not found in the conserved core photosynthetic genes but in genes encoding "auxiliary factors" or "modifiers" of photosynthesis (Flood et al., 2011). Thus, the use of natural variation to study the function of genes encoding for such regulators would be anticipated to provide further insight into the regulation of photosynthesis. Importantly, such regulators have not been identified in previous mutant screens. This is likely due to their redundancy, their large number, and the fact that individually they likely explain only a small fraction of the variance in photosynthesis.

Natural variation in plant growth has been described in a large number of species, including both the model plant *Arabidopsis* (Cross et al., 2006; Meyer et al., 2007; Sulpice et al., 2009) and crop plants (Driever et al., 2014; Liang et al., 2010; Rosado-Souza et al., 2015; Semel et al., 2006; Wen et al., 2016). However, like for photosynthesis, although these studies uncovered considerable natural variation in plant growth, relatively little is known concerning its genetic basis, possibly because the rate of growth is an integrator of numerous interdependent factors (Koornneef, Alonso-Blanco, & Vreugdenhil, 2004).

Higher rates of photosynthesis do not necessarily lead to increases in biomass and yield (Norby et al., 2006; Rossi et al., 2015). This can be explained by sink limitation and by variations in the regulatory networks of leaf metabolism. Indeed, several studies of natural genetic variation revealed a negative correlation between the levels of metabolites and biomass or yield (Cross et al., 2006; Meyer et al., 2007; Schauer et al., 2006). For example, in this context, a comprehensive study of 94 *Arabidopsis thaliana* ecotypes indicated that vegetative biomass is negatively correlated with many metabolites including starch, and that the regulatory network that determines metabolite levels contributes to the regulation of biomass production (Sulpice et al., 2009). Furthermore, a study using maize germplasm resources has expanded our knowledge of C and N metabolism in maize. This study allowed the identification of candidate genes involved in these metabolisms, such as a starch synthase and a ribosomal protein linked to chlorophyll *a* variation and biomass production, repectively (Zhang et al., 2015).

In tomato, numerous studies using wild species introgression line (ILs) populations have been performed in an attempt to understand tomato fruit composition (Do, Prudent, Sulpice, Causse, & Fernie, 2010; Frary et al., 2000; Fridman, Pleban, & Zamir, 2000; Liu et al., 2003; Quadrana et al., 2014; Schauer et al., 2006; Schilmiller et al., 2010; Tieman et al., 2006). Studies using the *Solanum pennellii* IL population (Eshed & Zamir,), have allowed the identification of hundreds of quantitative trait loci (QTL)-related to fruit traits (Semel et al., 2006), such as fruit metabolite composition (Almeida et al., 2011; Baxter et al., 2005; Causse et al., 2004; Fridman, Carrari, Liu, Fernie, & Zamir, 2004; Hackel et al., 2006; Schauer et al., 2006), fruit color (Liu et al., 2003), and enzymatic activities during fruit development (Steinhauser et al., 2011). This population has also been used to identify QTL involved in root and leaf morphology (Holtan & Hake, 2003; Chitwood et al., 2013; Ron et al., 2013), thus providing a large number of candidate genes (Kamenetzky et al., 2010). However, very few genes have been unambiguously cloned to date (de Godoy et al., 2013; Fridman et al., 2004; Quadrana et al., 2014; Ronen, Carmel-Goren, Zamir, & Hirschberg, 2000).

Traits related to photosynthesis, for example, morphological and anatomical determinants of mesophyll conductance have been studied in wild tomato species (Muir, Hangarter, Moyle, & Davis, 2014). In addition, QTL have been mapped in the *S. pennellii* IL population for leaf carbon isotope composition (Xu et al., 2008), leaf traits associated with adaptation to variation in water supply (Muir, Pease, & Moyle, 2014) and stomatal responsiveness, and g_s-related anatomical traits (Fanourakis et al., 2015). Thus, this extensively studied collection of ILs, associated with the recent availability of the genome sequence of the parental species (Bolger et al., 2014), constitutes a powerful tool for the identification of the genetic determinants involved in tomato physiology, growth, and development.

In this study, we determined photosynthetic traits in the *S. pennellii* IL population including a set of major leaf metabolites and growth-

related parameters. We identified QTL involved in the regulation of photosynthesis-related parameters and root and shoot dry matter accumulation, as well as in the levels of key primary metabolites. Furthermore, we performed genomic analyses of selected genomic regions and identified candidate genes for those traits. The results are discussed in the context of the importance of physiological and metabolic parameters in determining photosynthetic performance and plant growth. Moreover, multivariate analysis of the data set generated new insights in our understanding of the variation of physiological and metabolic traits, which are discussed in the context of the improvement of photosynthesis and plant growth in tomato.

2 | MATERIAL AND METHODS

2.1 | Plant materials and experimental conditions

S. pennellii ILs (Eshed & Zamir, 1995) and *Solanum lycopersicum* cv M82 seeds were kindly donated by Professor Dani Zamir, Hebrew University, Rehovot, Israel. The seeds were germinated on Murashige and Skoog media (Murashige & Skoog, 1962) containing 2% (*w*/*v*) sucrose and were grown in a growth chamber (250 μmol photons m^{-2} s^{-1}, 22 °C) for 45 days under a photoperiod of 16-hr-light/8-hr dark before transfer into the greenhouse. Rooted plantlets were acclimatized as described previously (Carrari et al., 2003) and subsequently transferred to 1.16 L pots containing commercial substrate Plantmax®, supplemented at the beginning of cultivation with 2.5 g chemical fertilizer (N:4; P_2O_5:14; K_2O:8) per pot. Plants were grown in a greenhouse located in Viçosa (642 m in altitude, 20°45′ S latitude and 42°51′ W longitude) in southeastern Brazil, under an average of 400 μmol photons m^{-2} s^{-1} daily light intensity. Throughout the growth period, the plants were maintained under naturally fluctuating conditions of light intensity, temperature, and relative air humidity. The experiment, comprising 71 ILs and M82, was repeated in spring of two consecutive years (2012 and 2013). M82 and ILs were arranged in randomized complete block design with six replicates (one plant per pot) considered as an experimental unit.

All sampling procedures were carried out on the first fully expanded source leaf of 4-week-old plants. Leaf samples for starch content were harvested at the end of night (EN), middle (MD) and end of day (ED). Plant growth was estimated using plant height (measured from the base to the tip of the terminal bud) and a time-component providing an integrative parameter referred to as relative growth rate (RGR) as described by (Hunt, 1982). The dry matter accumulated in shoot and roots was determined for each individual plant at the end of the experiment, 4 weeks after transfer to the greenhouse as described previously (Nunes-Nesi et al., 2005).

2.2 | Measurements of photosynthetic parameters

Gas-exchange analyses were performed on the second terminal leaflet of the third fully expanded leaf from the apex of 4-week-old plants using two identical portable open-flow gas-exchange systems (Li 6400XT, Li-Cor, Inc., Lincoln, NE, USA) equipped with an integrated fluorescence chamber (LI-6400-40; Li-Cor Inc.). Both devices were calibrated using exactly the same settings, and only one Li-COR machine was used per block. The net CO_2 assimilation rate (*A*), stomatal conductance to water vapor (g_s), and internal CO_2 concentration (C_i) were measured from 08:00 to 12:00 hr (solar time) under an external CO_2 concentration of 400 μmol mol^{-1} air, average temperature of 27 °C, and a flow rate of 300 μmol s^{-1} in both years. All measurements were conducted under an artificial, saturating light of 1,000 μmol photons m^{-2} s^{-1} that was provided by a light-emitting diode with 10% blue light in order to maximize stomatal opening. The rates of dark respiration were determined from 21:00 to 23:30 hr on the same leaf previously used to determine net carbon assimilation. From combined measurements of fluorescence and gas exchange, we estimated the photorespiration rate (*Pr*) according to Valentini, Epron, Angelis, Matteucci, and Dreyer (1995).

The same leaf previously used to determine *A*, was dark-adapted for 1 hr and illuminated with weak, modulated measuring beams (0.03 μmol m^{-2} s^{-1}) to obtain the initial fluorescence (F_0). Saturating white light pulses of 8,000 μmol photons m^{-2} s^{-1} were applied for 0.8 s to determine maximum fluorescence emission (F_m). In light-adapted leaves, the steady-state fluorescence yield (F_s) was measured and followed by a saturating white light pulse (8,000 μmol m^{-2} s^{-1}, 0.8 s) for determination of the light-adapted maximum fluorescence (F_m'). The actinic light was then turned off, and far-red illumination was applied (2 μmol m^{-2} s^{-1}) to measure the light-adapted initial fluorescence (F_0'; Aucique-Perez, Rodrigues, Moreira, & DaMatta, 2014). The values were used to determine the coefficients of photochemical quenching (*qP*) and non-photochemical quenching (*NPQ*) and the electron transport rate (*ETR*), as previously described (Aucique-Perez et al., 2014; Schreiber, Hormann, Neubauer, & Klughammer, 1995).

2.3 | Determination of metabolite levels

Leaf samples were harvested in the middle of light period or as indicated in the text and legend of figures, using the same leaf previously used to determine the photosynthetic parameters. The tissue was flash frozen in liquid nitrogen and stored at −80 °C until further analysis. Metabolite extraction was performed by grinding the tissue in liquid nitrogen followed by the immediate addition of 80% ethanol as described by Cross et al. (2006). The levels of starch, sucrose, fructose, and glucose in leaf tissue were determined exactly as previously described (Fernie, Roscher, Ratcliffe, & Kruger, 2001). The levels of malate was determined exactly as detailed by Nunes-Nesi et al. (2007), whereas nitrate (NO_3) and chlorophyll *a* and *b* contents were determined as detailed in Sulpice et al. (2009). Total protein and total amino acid contents were quantified as previously reported (Cross et al., 2006).

2.4 | Statistical analyses

Statistical analyses were performed using the GENES program (Cruz, 2013) and R statistical software (www.r-project.org). All data sets from 2012 to 2013 were subjected to a two-way analysis of variance, which was performed assuming random effects for blocks, genotypes, environment, and genotype *x* environment interaction. The linear model fit to the data was $Y_{ijk} = \mu + G_i + B_k + A_j + GA_{ij} + E_{ijk}$, where Y_{ijk} is the observed value of the *i*th line in the *k*th block and *j*th environment; μ

is the grand mean, G_i the random effect of line i; B_k the random effect of block k; A_j the random effect of environment j; GA_{ij} the random effect of the interaction of genotype i with environment j; and E_{ijk} is the experimental error. The means were tested by Dunnett's test at 5% significance level. Pearson correlation was performed for examining the relationships between variables. Pearson r values were converted to t values to obtain p-values. The resulting p-values were corrected using the Benjamini and Hochberg (1995) false discovery rate control, using an R script displayed by the Rbio software (www.biometria.ufv.br). For quantitative real time polymerase transcriptase (qRT-PCR) analyses, results were considered significant at $p \leq .05$, using the Student's t test available into Microsoft Excel.

2.5 | QTL analyses and the criteria for their selection

In this work, we defined QTL as those genomic regions for which a trait was significantly associated between the spanning IL and its recurrant parent (M82) by Dunnett's test ($p < .05$). The selection of the QTL-associated BINs for comparative genomic analyses was based on the criterion that the genomic regions were covered by at least two ILs displaying the same phenotypic variation from the parent M82.

2.6 | Gene annotation and analyses

Sequences of the selected region (Table S1) were retrieved from M82 and *S. pennellii* genomes (Bolger et al., 2014) by using the flanking markers (according to the IL genetic map deposited in the SOL Genomics Network portal) to blast both genome sequences as indicated in Table S2.

De novo gene prediction was performed by using Augustus software (Stanke, Steinkamp, Waack, & Morgenstern, 2004). Predicted proteins were functionally annotated by comparison against the SOL Genomics Network (http://solgenomics.net/) Heinz protein database and BLASTp engine with a cut off value of E-10. Proteins that matched transposable elements were removed from the data set.

Non-redundant gene lists for each BIN were extracted by a dedicated script and Mapman-categorized by using the published Mapman table Solyc ITAG 2.30 (http://solgenomics.net/) as subject. This was separately done for both M82 and *S. pennellii* genes. In order to assess over-representation of any Mapman category within the genomic regions analyzed, after categorization, a contingency table was built between the number of genes assigned to each category and those from the whole gene set of each plant species. Significance ($p < .05$) was tested using the Fisher test.

For candidate gene selection, the Blast2GO (Conesa et al., 2005) suite was utilized. The previously identified protein entries were used as queries for a BLASTp against the National Center for Biotechnology Information (NCBI) *A. thaliana* protein dataset with a cut-off value of E-3 and a maximum of 20 hits per sequence. Then, the GO terms were associated to each query based on the program annotation software, InterProScan, and ANNEX validation. Candidate genes were surveyed by biological process GO terms associated with the traits understudy. The GO terms analysed were malate transmembrane transport (GO: 0071423); carbohydrate metabolic process (GO: 0005975); photorespiration (GO: 0009853); photosynthesis (GO: 0015979); root system development (GO: 0022622); growth (GO: 0040007); cellular respiration (GO: 0045333); cell wall organization or biogenesis (GO: 0071554); and carbohydrate derivative metabolic process (GO: 1901135).

A survey of genes differentially expressed in the ILs was performed based on leaf RNA-seq data obtained from 76 tomato introgression lines that had been grown for 13 days (Chitwood et al., 2013). This published data set represents a major source of information and, therefore, was used to compare the expression levels of the selected candidate genes (Tables S3 and S4) across ILs and their possible association with phenotypic traits. Genes that showed changes in their expression levels and appeared associated to phenotypic traits were subjected to sequence analysis of the non-coding region upstream of their start codon ATG (up to around −1000 BP) from *S. lycopersicum* cv. M82 and *S. pennellii* genome sequences (Bolger et al., 2014).

2.7 | RNA extraction and qRT-PCR analysis

qRT-PCR analyses were performed for a subset of candidate genes in leaf samples harvested in the middle of light period; the same used for metabolite analyses. All procedure was performed as previously described (Caldana, Scheible, Mueller-Roeber, & Ruzicic, 2007). Gene expression values were normalized against the constitutively expressed ubiquitin and M82 parental line as described by Alseekh et al., 2013. Primers for all investigated candidate genes are described in the Table S5.

3 | RESULTS

3.1 | Natural variation of physiological and metabolic traits of the *S. pennellii* IL population

Phenotypic variation in terms of photosynthetic, metabolic, and plant growth-related traits was measured prior to flowering (Figure1). Overall, trait variation was largely similar between both experiments. However, as would be anticipated, large variability was observed between the two experiments for some traits (Figure 1; Tables S6 and S7), particularly for total amino acids, chlorophyll *b* content, NO_3, root dry weight (root DW), *ETR*, *qP*, and C_i.

3.2 | Pearson correlation analysis reveals interactions between physiological, metabolic and growth related traits

In order to provide an overview of the associations between traits, we built a network of all significant associations (Figure 2). The full dataset of correlation coefficients calculated in this study is presented as a heatmap in Figure S1. From this analysis 31 positive and 7 negative significant correlations were observed. Among them, some correlations were expected, such as the positive correlations observed between photosynthetic traits, for example, net CO_2 A and g_s ($r = .58$), g_s and C_i ($r = .79$), A and *ETR* ($r = .56$). Others were less intuitive, such as malate positively correlating with *ETR* ($r = .42$) and A ($r = .38$). Although A and g_s were positively correlated with *RGR* ($r = .33$ and .37, respectivelly); a direct correlation between A

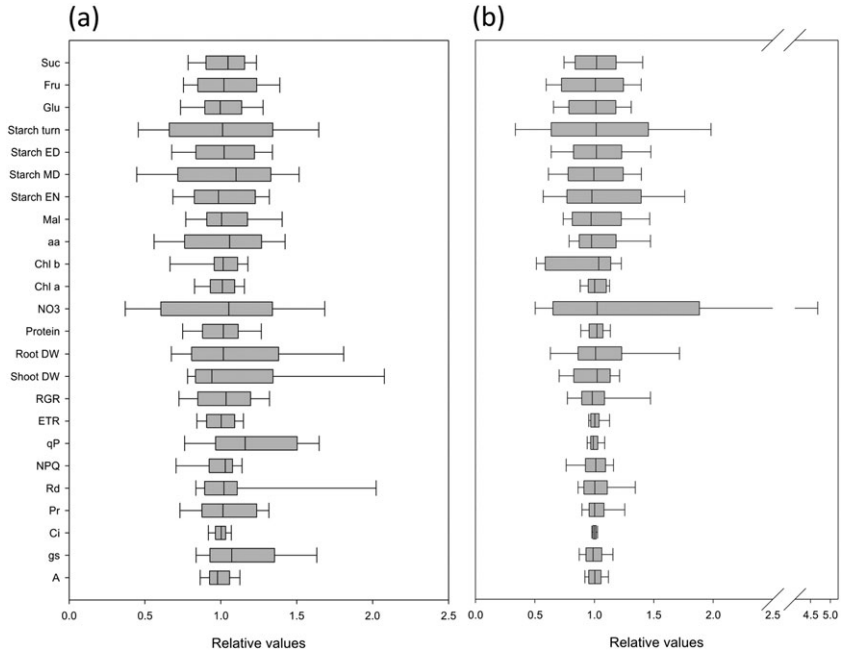

FIGURE 1 Boxplot graphs illustrating the changes in growth, physiological, and metabolic traits from the individual data sets of 2012 (a) and 2013 (b) of a population of 71 introgression lines of *Solanum pennellii* into a genetic background of *Solanum lycopersicum* (M82). Gas exchange and chlorophyll *a* fluorescence parameters: photosynthesis (*A*), stomatal conductance (g_s), intercellular CO_2 concentration (C_i), photorespiratory rate (Pr), dark respiration (Rd), non-photochemical quenching (NPQ), photochemical quenching (qP), and electron transport rate (ETR). Growth related parameters: relative growth rate (RGR), shoot dry weight (Shoot DW), and root dry weight (Root DW). Nitrogen and carbon containing compounds in leaves: malate (Mal), glucose (Glu), fructose (Fru), sucrose (Suc), chlorophyll *a* (Chl *a*), chlorophyll *b* (Chl *b*), protein, amino acid (aa), NO_3, starch levels at the end of the night (Starch EN), middle of the day (Starch MD), end of the day (Starch ED), and starch turnover (starch turn). Except for starch data, samples were harvested at the middle of the light period. The median is indicated by solid lines in each box. Data are normalized to the median of each trait

or g_s with dry matter accumulation in shoots was not observed. However, C_i was negatively correlated with dry matter biomass in shoots (r = −.40), suggesting that the internal CO_2 leaf concentration is a key trait for efficient carbon assimilation. Although no correlation between *A* and photorespiratory rate (*Pr*) was observed; *ETR* and *qP* were positively correlated with *Pr* (r = .92 and .61; respectively), suggesting that *Pr* might be an important process involved in the dissipation of light energy that cannot be assimilated by the Calvin–Benson cycle.

Positive correlations between sugar and starch content at ED, EN, and midday were observed (Figure S1). Here, starch turnover correlated negatively with starch content at EN (r = −.39) but positively with starch content at MD (r = .36) and ED (r = .63). Starch content at MD also correlated negatively with shoot DW (r = −.35), although total amino acid content correlated positively with root DW and shoot DW (r = .40 and .39; respectively).

3.3 | Identification of QTL for leaf photosynthetic, metabolic and plant growth-related parameters

QTL were defined as genomic regions for those traits where a two-way analysis of variance modelling genotype and year (Table S8) displayed a significant effect (p < .05) for the genotype. These were further filtered to only comprise those QTL with a significant genotype effect, when the difference between any IL and its recurrent parent (M82) was also significant when tested by Dunnett's post-hoc test at 5% significance level. Using this criterion, we identified 208 single-trait QTL (Figure 3). Of the photosynthetic parameters, *A* had the most complex genetic architecture with 16 ILs exhibiting higher *A*. In contrast, only five QTL for g_s, one QTL for NPQ, qP and Pr and two for C_i, *ETR*, and rates of dark respiration were identified (Figure 3). Regarding plant growth related traits, we identified five QTL for higher and eight for lower dry matter accumulation in shoots and two QTL for higher and 34 for lower root DW. Thirty-nine QTL for nitrogen metabolism were identified including 14 for nitrate content, seven for chlorophyll *b*, and nine for total amino acid contents. Regarding carbon metabolism, we identified six QTL for malate levels, 36 for starch levels, and 16 for starch turnover. Seven, twenty-one and one QTL were observed for glucose, fructose, and sucrose leaf contents, respectively.

3.4 | Identification and characterization of BINs

In order to map the identified QTL to smaller interval, termed BINs, we identified the overlap between the introgressed regions of the ILs and the traits showing significant differences in comparison to the control M82 (Figure 3, Table 1). The criterion to select the QTL-associated BINs for further comparative genomic analyses was that the regions were covered by at least two ILs displaying the same phenotype. We used this criterion to narrow down the number of genes, even though common associations between two overlapping ILs could also be explained by different genes present in non-overlapping regions of the ILs. By applying this criterion, we identified 41 QTL-associated BINs distributed in 33 overlapping regions (Figure 3 and Table 1). Furthermore, we focused on 11 of these BINs (Table 2), which showed highly significant physiological and metabolic changes, for further genomic analyses, namely, (a) candidate gene identification and (b) analyses of their genomic contexts (Tables S1 and S9). Out of the 11 BINs, only four, 2C, 4A, 9C, and 11D, displayed the same number of

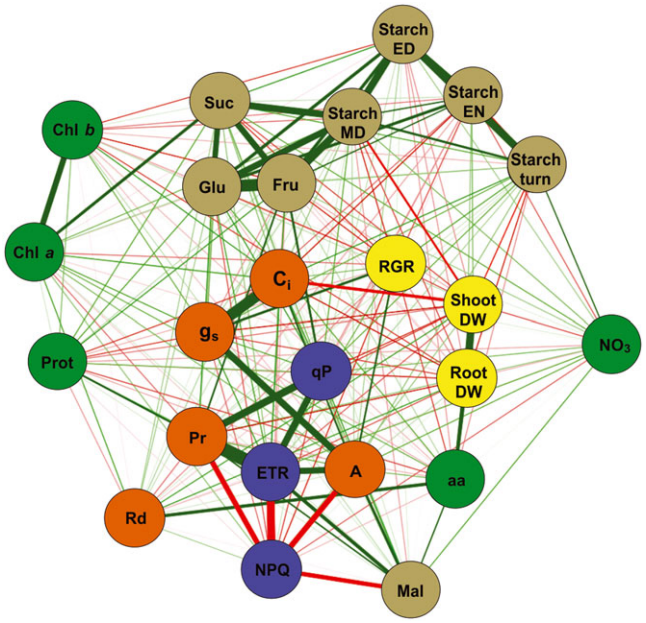

FIGURE 2 Correlation network based on Pearson coefficients derived from the average data obtained in 2012 and 2013 from a population of 71 introgression lines of *Solanum pennellii* into a genetic background of *Solanum lycopersicum* (M82). Trait associated with gas exchange are shown as beige dots; chlorophyll *a* fluorescence in lilac dots; growth related parameters in yellow dots; nitrogen metabolite in green coloured; and carbono metabolite brown coloured. Green and red connecting lines represent positive and negative correlations, respectively. Line width is proportional to the strength of the correlation. Gas exchange and chlorophyll *a* fluorescence parameters: photosynthesis (A), stomatal conductance (g_s), intercellular CO_2 concentration (C_i), photorespiratory rate (Pr), dark respiration (Rd), non-photochemical quenching (NPQ), photochemical quenching (qP), and electron transport rate (ETR). Growth related parameters: Relative growth rate (RGR), shoot dry weight (Shoot DW), and root dry weight (Root DW). Nitrogen- and carbon-containing compounds in leaves: malate (Mal), glucose (Glu), fructose (Fru), sucrose (Suc), chlorophyll a (Chl *a*), chlorophyll b (Chl *b*), protein (Prot), amino acid (aa), NO_3, starch levels at the end of the night (Starch EN), middle of the day (Starch MD), end of the day (Starch ED), and starch turnover (Starch turn)

predicted gene *loci* in the two parental species. In total, 1,676 (15%) more *S. pennellii* than M82 *loci* were detected among the BINs, with BIN 3D and 4DE exhibited 47% and 12% more *loci* for *S. pennellii* than M82 (Table 1).

Mapman annotation revealed a wide distribution of categories in all of the selected BINs (Table S10). All categories occurred in more than one analyzed genomic region with the exception of Category 6 (gluconeogenesis/glyoxylate cycle) that appeared only in BIN 11B that harbours a QTL for starch content in leaves at the end of the day. The diversity of Mapman categories found in our analysis denotes a broad range of function for the genes spanning these genomic regions (Table S10). However, when a further over-representation analysis followed by a Fisher test was performed; results suggest that a considerable number of categories are over-represented within the genomic regions analyzed and that, in certain regions, functional categories are differentially represented between the two parental genotypes (Table 2).

3.5 | Identification of candidate genes

By Blast2GO annotation and the selection of all GO terms related to the traits, we analyzed (see Section 2) a list of 87 candidate genes (Table S4; see Table S1 for all genes present in the BINs) was generated. Most of these candidates are encoding for enzymes (31) or genes involved in receptor/signaling processes (18). However, a number of them are also involved in RNA metabolism or associated with transport. With the exception of BINs 9D (*S. pennellii*) and 11B (both genotypes), more than 50% of the candidate genes selected belong to one over-represented Mapman category, whereas the only candidate selected from BIN 11D does not (Figure S2).

The identity between the predicted proteins of *S. lycopersicum* (M82) and *S. pennellii* varied between 80% and 100% with only four proteins predicted to be identical in length and amino acid sequence (Tables S9 and S4). Out of the 73 polymorphic proteins, 41 displayed differences in length. Interestingly, two and seven genes were exclusively present in *S. lycopersicum* or *S. pennellii*, respectively (Table S4).

3.6 | Expression and sequence analysis of candidate genes

In order to verify if the 87 identified candidate genes displayed changes in the amount of mRNA between their *S. pennelli* and *S. Lycopersicon* alleles, we checked their expression levels in the leaves of the ILs, using published RNA-seq data (Chitwood et al., 2013; Table S3). A subset of 30 out of our 87 (34%) candidate genes showed significant changes in the mRNA accumulated in leaf cells when comparing the *S. pennellii* with the *S. lycopersicum* alelles (Table S3). Interestingly, when assessing for the difference in expression of all genes present within the BINs, 11 additional genes showed significant changes between the *S. pennellii* and *S. lycopersicon* alleles. Thus, the validity of our targeted approach using biological function as a proxy for identifying candidate genes is confirmed by an untargeted approach using significant changes in expression as a criterion. It is important to note, however, that caution should be taken as not to over-interepret this comparison given that the RNAseq data were obtained from an entirely independent experiment and solely for leaves.

In order to investigate possible mechanistic explanations for the expression QTL mentioned above, we further performed comparative analyses of the regulatory regions from those genes showing transcriptional differences between both alleles. In BIN 11H, where a QTL for high *A* rate was detected, a mitogen-activated protein kinase encoding *locus* (Solyc11g072630) showed mRNA changes in the two overlapping lines spanning this region (IL 11-4 and IL11-4-1) in comparison to other lines harbouring the *S. lycopersicum* allele (Table S3). Sequence analyses of the anti-thymocyte globulin upstream region revealed three InDels of 14 to 36 nt in length, in addition to several smaller ones.

In IL 9-1 (BIN 9C), the up-regulation observed in the expression of the pyruvate kinase gene (Solyc09g008840) could be associated with higher amino acid content and shoot DW. A sequence alignment between M82 and *S. pennellii* at the upstream region showed six InDels ranging in length between 7 to 26 BP. On the other hand, the expression level of the glucose transporter (Solyc09g074230), located in BIN 9G where an association for root DW had been detected, was

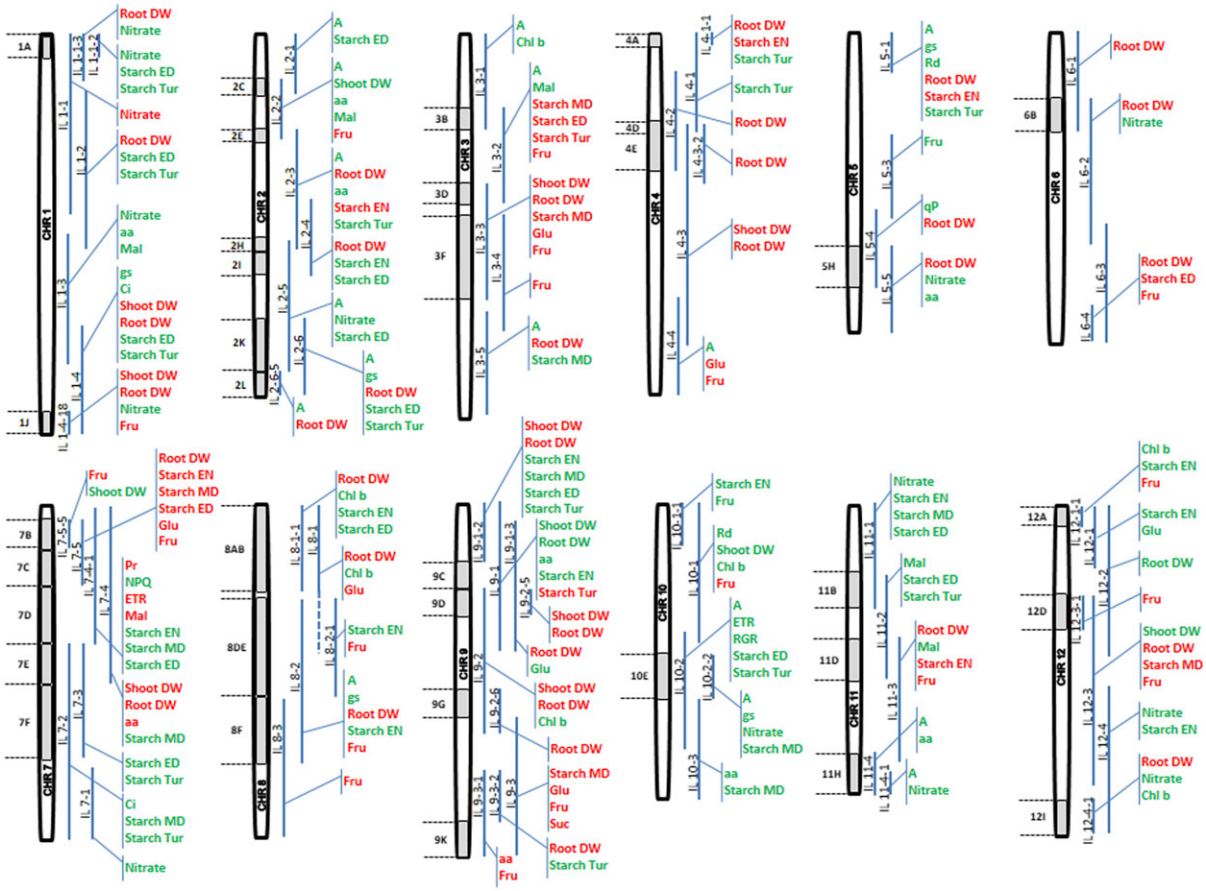

FIGURE 3 Quantitative trait locus map of significant changes conserved for the growth, physiological, and metabolic traits in both seasons (2012 and 2013) of a population of 76 introgression lines of *Solanum pennellii* (blue bar) into a genetic background of *Solanum lycopersicum* (M82). Gas exchange and chlorophyll *a* fluorescence parameters: photosynthesis (A), stomatal conductance (g_s), photorespiratory rate (Pr), dark respiration (Rd), intercellular CO_2 concentration (C_i), non-photochemical quenching (NPQ), electron transport rate (ETR); relative growth rate (RGR), shoot dry weight (Shoot DW), and root dry weight (Root DW). Nitrogen and carbon containing compounds in leaves: malate (Mal), fructose (Fru), sucrose (Suc), glucose (Glu), chlorophyll *b* (Chl b), amino acid (aa), starch levels at the end of the night (Starch EN), middle of the day (Starch MD), end of the day (Starch ED), and starch turnover (Strach tur).Traits indicate a positive (green) or negative (red) significant changes as compared to M82 as identified by Dunnett's test. Grey bars represent the 33 overlap regions from 41 QTL-associated BINs annotated [Colour figure can be viewed at wileyonlinelibrary.com]

lower in the overlapping IL9-2 and IL9-2-6 compared to other lines. A very low similarity between M82 and *S. pennellii* sequences upstream of the protein coding region of this gene was observed with a large InDel of around 100 BP.

A QTL for higher starch accumulation at ED was mapped to BIN 11B co-locating with the Solyc11g010290 *locus* encoding a 2-oxoglutarate/malate translocator. When inspecting the mRNA accumulation of this gene, a twofold higher expression was observed in ILs harbouring the *S. pennellii* allele (IL 11–1 and IL11–2) in comparison with those harbouring the *S. lycopersicum* one (Table S3). Sequence alignments of the upstream region revealed the presence of five InDels of 3 to 16 nt in length, in addition to several single-nucleotide polymorphisms.

3.7 | qRT-PCR analyses for candidate genes associated with high assimilation rate, biomass production, and carbon metabolism

In order to provide further evidence for those genes identified as candidates, we assessed the expression of 20 of them by quantifying their mRNA levels by qRT-PCR. These genes were selected based on their close association with the evaluated leaf traits. Specifically, we selected the genes in BINs associated to *A*, biomass production, and starch accumulation. Out of the 20 selected genes, eight showed a significant change in their mRNA accumulation levels between their *S. pennelii* and M82 alleles (Figures 4 and S3). In the genomic region of BIN 2 K, where a QTL for *A* and starch levels at the end of the day was mapped, significant reductions of the mRNA from the *S. pennellii* alleles were detected for those *loci* encoding a adenosine triphosphate (ATP)-dependent Clp protease, a nicotinamide adenine dinucleotide (NADH) dehydrogenase, the iron–sulphur subunit of the succinate dehydrogenase enzyme (significant for IL 2-6), and the beta subunit of an ATP synthase of the F1 complex (Figure 4a). For the other two assessed genes, a serine hydroxymethyltransferase and a pro-apoptotic serine protease, we were not able to detect any QTL in the leaves of the tested ILs (Figure 4a). In addition, we also checked the expression of three other candidates mapped to another QTL for *A* on BIN 11H; a mitochondrial F_0 ATP synthase encoding gene appears as an QTL with significant reduced levels of the *S. pennellii* allele

TABLE 1 Gene content of analysed BINs

		Number of predicted *loci*[b]	
Trait[a]	BIN	*Solanum lycopersicum*	*Solanum pennellii*
A	2C	1	1
	2H	166	177
	3B	44	49
	10E	319	324
	11H	62	68
A and aa	2E	163	168
A and starch ED	2 K	138	149
A and root DW	2 L	125	130
Root DW	4DE	1140	1292
	5H	95	104
	6B	249	280
	7 BC	263	262
	9D	54	56
	9G	74	76
Root and shoot DW	1 J	202	208
	9C	75	75
Root DW and Chl *b*	8AB	3461	3942
Starch ED	2I	305	314
	11B	100	104
Starch MD	7E	472	449
Starch EN	12A	117	127
Starch turn	4A	0	0
	7F	168	165
Starch MD and Fru	3D	1808	2663
Starch EN and Fru	8DE	505	516
Mal	11D	17	17
Nitrate	1A	64	70
	12I	21	24
Fru	3F	380	393
	7B	279	291
	8F	122	126
	9 K	120	119
	12D	303	349

Note. ED = end of the day; MD = middle of the day; DW = dry weight; Fru = fructose; Mal = malate; Chl *b* = chlorophyl *b*; aa = amino acid; A = photosynthesis.

[a]Trait abbreviation are according to Figure 2.

[b]The complete list of the predicted loci and their corresponding gene annotations are presented in Table S3.

(Figure 4b). The other two genes (a mitogen-activated and a serine–threonine protein kinases) did not show significant differences in their mRNA levels in the leaves of any of the tested ILs (Figure 4b). Furthermore, we also checked the expression of five candidate genes proposed to be involved in the regulation of the shoot and root DW QTL mapped at BIN 9C. The expression of a pyruvate kinase was significantly increased in the two IL harbouring the *S. pennellii* allele (Figure S3a). The other four genes (Solyc09g008640, Solyc09g008490, Solyc09g009190, and Solyc09g008480) did not show consistent changes in their expression when comparing ILs containing the domesticated and the wild alleles (Figure S3a). Candidate genes for leaf starch content at end of day QTL were assessed also for their expression levels in leaves samples at middle of the light period. In the BIN spanning this QTL, three genes were found to harbour expression QTL with the wild allele resulting in reduced expression levels, namely, a beta-glucosidase, a 2-oxoglutarate/malate translocator, and a pyrophosphate-dependent phosphofructokinase (Figure S3b). However, the other three of the candidates selected for this genomic region showed no differences in their mRNA accumulation levels (Figure S3b).

4 | DISCUSSION

4.1 | Variance in gas exchange and fluorescence in the *S. pennellii* IL population

Sixteen *S. pennellii* ILs displayed higher, but no ILs displayed lower, *A* (Figure 3). This is surprising because *S. pennellii* was previously reported to display a lower *A* than *S. lycopersicum* when grown under similar conditions to those reported here (Carrari et al., 2003; Nunes-Nesi et al., 2005). This suggests a relatively complex genetic architecture of photosynthetic performance in tomato. In the present study, we measured increases in *A* of up to 19%. This is in the range of the increases reported using transgenic approaches in tobacco over-expressing both sedoheptulose-1,7-bisphosphatase fructose-1,6-

TABLE 2 Differentially over-represented Mapman categories in the analyzed genomic regions from *Solanum pennellii* and *Solanum lycopersicum*

BIN	Trait	Over-represented Mapman category (BIN code)	*Solanum pennellii* Count	*p*-value*	*Solanum lycopersicum* Count	*p*-value*
1 J	Root and shoot DW	Development (33)			13	.032
		Polyamine metabolism (22)	2	.013		
		Miscellaneous (26)	22	.038		
2 L	*A* and root DW	Biodegradation of xenobiotics (24)			2	.011
		Miscellaneous (26)	16	.021		
4DE	Root DW	Signalling (30)			78	.047
9G		RNA (27)	18	.016		
		Stress (20)	8	.024		
7 BC		Major CHO metabolism (2)			6	.025
		Lipid metabolism (11)			10	.036
		Photosynthesis (1)			9	.049
2 K	*A* and starch ED	Cell wall (10)			7	.047
		Minor CHO metabolism (3)	4	.014		
11H	*A*	Metal handling (15)	2	.019		
9D	Root and shoot DW	TCA/organic transformation (8)	2	.011		
11B	Starch ED	Amino acid metabolism (13)	5	.016		
		Not assigned (35)	12	.046		
11D	Malate	Metal handling (15)			2	.001
		RNA (27)	6	.018		

Note. The BIN 9C is not showed, once it is not was differentially over-represented in the analyzed genomic regions from *Solanum pennellii* and *Solanum lycopersicum*. DW = dry weight; A = photosynthesis; CHO = carbohydrates; TCA = tricarboxylic acid cycle; Starch ED = starch levels at the end of day; RNA = ribonucleic acid.

*Over-representation was assessed as described in the Material and Methods section and signifance level was tested by a Fisher's test ($p < .05$).

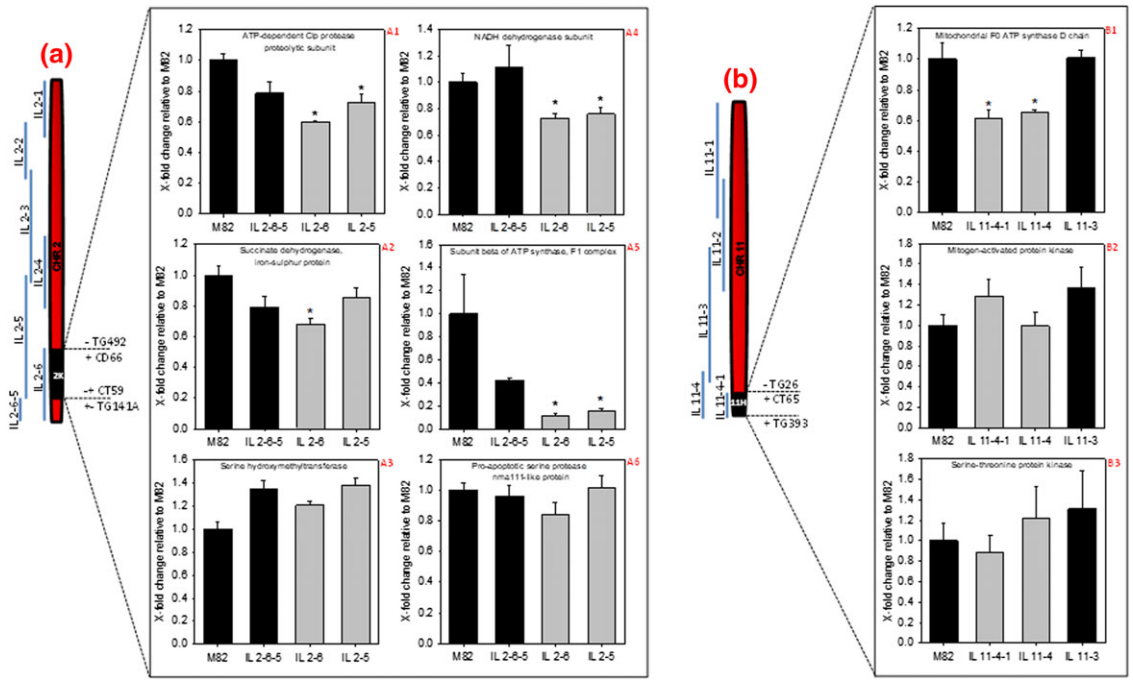

FIGURE 4 Quantitative real-time polymerase chain reaction expression analysis of nine candidate genes present in BIN 2 K (A1–A6) and BIN 11H (B1–B3). Values are mean of four biological replicates and are represented as fold changes compared to M82. The assigned functions and primers used for quantitative real-time polymerase chain reaction are provided in the Table S5. Bars represent ±*SE* and asterisks indicate a significant difference at $p \leq .05$. The grey bars represent introgression lines where harbour an allele of *Solanum pennellii* [Colour figure can be viewed at wileyonlinelibrary.com]

bisphosphate aldolase and ictB (19%; Simkin, McAusland, Headland, Lawson, & Raines, 2015), and tomato down-regulated in the expression of the mitochondrial malate dehydrogenase enzyme (25%; Nunes-Nesi et al., 2005). A strong positive correlation between g_s and malate with *A* was observed (Figure 2 and Figure S1), suggesting that the higher *A* observed in some ILs was partially related to stomatal movement. Recent evidence indicates that malate plays a key regulator role in stomatal function (Araújo et al., 2011; Gago et al., 2016; Medeiros et al., 2015; Nunes-Nesi et al., 2007). In addition, the identification of many QTL involved in traits related to g_s have been reported

(Fanourakis et al., 2015; Frei, Tanaka, & Wissuwa, 2008; Khowaja & Price, 2008; Muir et al., 2014; Price, Young, & Tomos, 1997; Xu et al., 2008). Recently, using a subset of the same IL population, the variation in stomatal responsiveness to desiccation and g_s-related anatomical traits under well-watered conditions was assessed (Fanourakis et al., 2015). Interestingly, ILs 1-2, 2-6, 2-6-5, and 3-1 displayed increased in g_s. Given that three of these four ILs (IL 2-6, 2-6-5, and 3-1) also showed higher *A* and 43.8% of the photosynthetic QTL identified by us also displayed some variation in stomatal response or anatomical characteristics (Fanourakis et al., 2015), this provides support for the conclusion that stomatal variation has a large influence on photosynthetic rates in tomato.

We additionally identified a negative correlation between C_i and shoot DW (Figure S1). Lower C_i can be expected under water limited environments in order to provide long-term benefits (Jackson et al., 2016). However, under well-watered conditions, lower C_i may arise from either increased photosynthetic capacity or as a response of g_s to genetic differences in leaf anatomy (Condon, Richards, Rebetzke, & Farqhuar, 2004; Fanourakis et al., 2015). Therefore, it seems reasonable to assume that both processes might impact plant growth and yield in a species dependent manner. In the experiment reported here, it is possible to infer that low C_i is likely due to changes in g_s, because positive correlations between g_s and C_i were observed. Although most of the photosynthetic variation has been explained by variations in g_s, previous studies have reported that several segments of the *S. pennellii* genome, when introgressed into the *S. lycopersicum* background, resulted in changes in carbon isotope composition ($\delta^{13}C$) relative to M82 (Xu et al., 2008). In their study, Xu et al. found that the line IL 5-4 displayed the least negative $\delta^{13}C$, corresponding the greatest water use efficiency and that several other ILs had more negative $\delta^{13}C$ than M82, including IL2-3, IL2-4, IL12-2, IL3-5, IL7-2, and IL9-2. They also found that IL 11-4 displayed a higher $\delta^{13}C$ than M82. Interestingly, this line, together with the overlapping line (IL 11-4-1), displayed an elevated *A* in our study.

Chlorophyll fluorescence related traits are sensitive indicators of uptake, use, and dissipation of photosynthetically active radiation, and therefore, changes in chlorophyll fluorescence emissions are related to the photosynthetic performance (Baker & Rosenqvist, 2004). In tomato growing under chilling stress, two QTL affecting non-photochemical quenching were detected, and one QTL associated with both photochemical quenching and F_v/F_m were identified, all on chromosome 5 (Oyanedel, Wolfe, Owens, Monforte, & Tanksley, 2000). In the present study, only three IL (IL 5-4, IL 7-4-1 and IL 10-2) displayed significant differences in fluorescence parameters, but only one of these also displayed variation in *A* (Figure 3). However, positive correlations were observed between *ETR* and *NPQ* with *A* (Figure 2). Thus, these results indicate that the higher photosynthetic rates observed in some of the ILs might also be associated with changes in photochemical reactions. Interestingly, *NPQ* negatively correlated with malate levels, and both traits are co-located in the same genomic region delimited by the IL 7-4-1 (Figures 2 and 3). Similar correlations have been observed in *Capsicum chinense* (Rosado-Souza et al., 2015). Despite the fact that there is no correlation of *Pr* with *A*, strong positive correlations of *qP* and *ETR* with *Pr* were observed in this study (Figures 2 and S1). This suggests that *Pr* is an important process to maintain the balance between *A* and light reactions in tomato plants and its increase impacts growth rates of this species. Accordingly, it is known that *Pr* can act as a sink for excess of reducing power in plants under abiotic stress conditions (Kangasjärvi, Neukermans, Li, Aro, & Noctor, 2012), such as high-light stress (Takahashi, Bauwe, & Badger, 2007).

4.2 | Trade-off between leaf metabolism and growth-related parameters

Among the metabolic parameters measured, sugar and starch showed the highest number of QTL distributed over the 12 chromosomes of tomato. QTL for sugar content have previously been identified in tomato fruit (Baxter et al., 2005; Eshed & Zamir, 1995; Fridman et al., 2004). In the present study, we identified seven negative QTL-associated BINs for fructose (Figure 3). This is in agreement with previous studies reporting that sucrose and fructose levels are considerably lower in leaves of all wild tomato species (Schauer, Zamir, & Fernie, 2005). Additionally, considering that leaves are the source of most fruit photoassimilates (Lytovchenko et al., 2011) and that overwhelming evidence suggests that sugars are apoplastically unloaded from the phloem into the fruit (Fridman et al., 2004; Hackel et al., 2006), these changes in leaf sugar levels would be expected to influence sugar levels in fruits. By comparing our data with those reported by Schauer et al. (2006), it appears that the link is not clear. The IL4-4 and IL5-1, showing higher *A* in leaves, have been found to have enhanced accumulation in several amino acids, sugars, and organic acids in fruits. However, other two lines (IL11-4 and 11-4-1 and BIN 11H), with higher *A* did not displayed a changes in any of the 74 metabolic traits evaluated by Schauer et al. (2006). A further 12 lines showing higher *A* in our study have previously showed significant changes in only a few fruit metabolites. Although such comparisons should strictly be made on the same plants, taken together these results indicate that an increase in *A* would likely only have a minor effect on fruit composition.

We additionally identified 36 QTL for root DW and 13 QTL for shoot DW (Figure 3). However, no consistent co-localization was found between *A* and shoot DW when all ILs were compared (Figure 3). This likely reflects the fact that shoot biomass is a very complex trait that involves numerous small effect QTL underlying genes involved not only in photosynthesis but also in the usage of photosynthetates, the regulation of meristematic activity, cell expansion, and architecture of the plant (Demura & Zheng-Hua, 2010). Given that the experiments were carried out using relatively young plants prior to flowering, it was not entirely possible from this study to directly assess the link between *A* and fruit yield. That said, fruit yield for this population has been measured in several previous studies and is highly robust across harvests (Semel et al., 2006). Interestingly, in Semel et al. (2006), the lines IL 2-5 (plant weight and fruit number), 2-6 (plant weight and fruit number), 3-5 (biomass, plant weight, and fruit number), 11-4 (plant weight and fruit number), and 11-4-1 (plant weight and fruit number) had significantly higher yield related traits, and these lines also showed a higher *A* in our study (Figure 3).

4.3 | Structure and expression of selected candidate genes

We further selected genes based on biological processes associated with the traits understudy (Table S4). The candidate genes were surveyed for their protein sequence identity and gene expression levels in *S. pennellii* and *S. lycopersicum* orthologs (Table S3). Based on leaf expression data from a previous study (Chitwood et al., 2013), we could show that 30 out of 87 of our candidate genes displayed significant changes in expression between *S. pennellii* and *S. lycopersicon* alleles (Table S3). Further qRT-PCR analyses confirmed that 40% of these genes to be differentially expressed for their *S. lycopersicon* and *S. pennellii* alleles (Figures 4 and S3). Concerning the two QTL for high assimilation rates (BIN 2 K and 11H), we investigated three genes from BIN 2 K and one from BIN 11H. In BIN 2 K, we found that a gene encoding an ATP-dependent Clp protease was differentially expressed (Figure 4). In silico analysis indicates that this gene is highly expressed in tomato leaves, and the *Arabidopsis* homolog is located in the chloroplast stroma (Adam & Clarke, 2002). It has been shown that the *A. thaliana* Clp protease, ClpP6, is important for chloroplast development, via the degradation of different regulatory proteins and metabolic enzymes impacting photosynthesis (Sjögren, Stanne, Zheng, Sutinen, & Clarke, 2006). In the same genomic region, two other genes involved in energy metabolism were identified; a NADH dehydrogenase iron–sulfur protein 4, a subunit of mitochondrial complex I, and a beta subunit of an ATP synthase (Figure 4). In tomato plants, NADH dehydrogenase iron–sulfur protein 4 is less expressed in leaves but has higher expression in mature fruits and flower buds. Moreover, it has been shown that Complex I represents a major entry site for electrons into the respiratory chain, transferring electrons from NADH to ubiquinone (Braun et al., 2014). Furthermore, Complex I subunits might play different roles in photosynthesis (Meyer et al., 2009; Noctor, Dutilleul, De Paepe, & Foyer, 2004). The second gene (the beta subunit of an ATP synthase) also has lower expression in tomato leaves and is highly expressed in flower buds and fruits. A third candidate gene also annotated as an ATP synthase subunit was identified in the genomic region 11H (Figure 4). This gene is highly expressed in tomato leaves and in early developmental stage of flowers and fruit tissues. The importance of ATP synthase in plants has been very well demonstrated. Short-term inhibition of ATP synthase by oligomycin gradually decreases the cellular ATP/adenosine diphosphate ratio and lead to transcriptional reprogramming, which consists of an early and massive induction of alternative respiratory pathways (Geisler et al., 2012). Moreover, genetic studies provided further support for the importance of the enzyme in plants, with mutants of the δ-subunit of mitochondrial ATP synthase in *Arabidopsis* leading to long-term adjustments in mitochondrial metabolism, reduced growth, and deficient gametophyte development (Geisler et al., 2012).

In addition, our analyses point out two glycolytic enzymes; pyruvate kinase (Solyc09g008840; on BIN 9C) and pyrophosphate-dependent phosphofructokinase (Solyc11g010450 on BIN 11B) for shoot and root DW and starch accumulation at ED, respectively (Figure S3). In tobacco plants, deficient in leaf cytosolic pyruvate kinase, an altered regulation of sink-source metabolism, was observed (Grodzinski, Jiao, Knowles, & Plaxton, 1999; Knowles et al., 1998). In tomato, pyruvate kinase is highly expressed in flowers, during anthesis, fruit set, and in fruits. In agreement with the studies on tobacco, we observed higher expression levels for this gene in the ILs harbouring the *S. pennellii* allele that is related with increase in shoot and root DW, suggesting that this enzyme might be related with carbon partitioning (Figure S3). The second glycolytic enzyme, pyrophosphate-dependent phosphofructokinase [Solyc11g010450; Diphosphate—fructose-6-phosphate 1-phosphotransferase (PFP)], is present in BIN 11B and associated with high starch at ED (Figure S3). This candidate gene is highly expressed in fruits and flowers and less in roots and leaves. PFP has been well characterized in a range of plant species at the biochemical and molecular level (Mustroph, Sonnewald, & Biemelt, 2007). In transgenic potato plants with strong reduction in PFP activity, it appeared that PFP had a very low flux control coefficient on glycolysis (Hajirezaei et al., 1994). However, PFP seems to be involved in adaptation of plants to stress conditions (Mertens, Larondelle, & Hers, 1990). Our results indicate that PFP activity might be associated with the higher starch levels observed in the ILs covering the BIN 11B.

In BIN 11B, we identified two more candidate genes; a beta-glucosidase and a 2-oxoglutarate/malate translocator (Figure S3). This beta-glucosidase gene in tomato is highly expressed in roots, red, and breaker fruits and less expressed in leaves. In plants beta-glucosidases are involved in a large number of biological functions, including defense, symbiosis, cell wall catabolism and lignification, signaling, and plant secondary metabolism (Cairns & Esen, 2010). It has been shown that putative beta-glucosidase encoding genes are induced by stresses and are necessary for stress tolerance (Lipka et al., 2005; Malboobi & Lefebvre, 1997). However, the precise role of these enzymes depends on their substrate-specificities, their tissue, and subcellular localization and conditions (Cairns & Esen, 2010). The second candidate gene on BIN 11B is annotated as a 2-oxoglutarate/malate translocator, which mediates the transport of 2-oxoglutarate produced in the cytosol or the mitochondrion into the chloroplast in counter exchange for malate, thus, providing the 2-oxoglutarate required for ammonia assimilation by the plastidic glutamine synthetase/glutamate synthase (Eisenhut, Hocken, & Weber, 2015; Schneidereit, Häusler, Fiene, Kaiser, & Weber, 2006). *I*n silico analysis indicates that the gene is highly expressed in tomato leaves, stems, and seedlings and during fruit set. It has been shown that the 2-oxoglutarate/malate translocator plays an important role at the interface between carbon and nitrogen metabolism in tobacco leaves (Schneidereit et al., 2006) and is important for storage proteins and amino acid biosynthesis in pea seeds (Riebeseel et al., 2010). These findings point to a crucial role of 2-oxoglutarate/malate translocator in carbon metabolism and in particular the regulation of starch content.

5 | CONCLUDING REMARKS

The current study is, to our knowledge, the largest study of photosynthetic gas exchange, growth, and metabolic parameters in tomato leaves to date. Importantly, our results demonstrate significant natural variation in photosynthetic, growth, and essential metabolites (C and

N) between tomato introgression lines. In this study, we identified 208 QTL for *A*, g_s, starch metabolism, root and shoot dry matter accumulation, and metabolites. Further, genomic analysis from 11 BINs allowed us to pinpoint 87 candidate genes that might regulate these traits. Interestingly, we did not detect co-association at any *loci* between *A*, g_s, *ETR*, and RGR hinting that a highly complex genetic architecture underpins photosynthesis. This study, together with previous studies on the same population that allowed the identification of QTL for gene expression, metabolite, and enzyme activity, pave the way towards the validation of candidate genes regulating photosynthesis related traits in tomato. In summary, this study provides an invaluable resource for progressing towards the mechanistic basis of how sequence variants affect photosynthesis and ultimately growth. Furthermore, we provide the basic foundation for the improvement of photosynthetic capacity and yield, aiding in our current understanding of the physiological and biochemical mechanisms involved in the regulation of primary metabolism in tomato leaves.

ACKNOWLEDGMENTS

Financial support was provided by Conselho Nacional de Desenvolvimento Científico e Tecnológico (CNPq) (Grant 484675/2013-3 to A. N. N. and 401090/2014-0 to R. S. and F. M. D.), Fundação de Amparo à Pesquisa do Estado de Minas Gerais (FAPEMIG) (Grant APQ-00688-12, APQ-02548-13, and BDS-00040-14) and Max Planck Society to A. N. N. and W. L. A.. Research fellowships granted by CNPq to A. N. N., F. M. D. and W. L. A. are also gratefully acknowledged.

ORCID

Adriano Nunes-Nesi http://orcid.org/0000-0002-9581-9355

REFERENCES

Adam, Z., & Clarke, A. K. (2002). Cutting edge of chloroplast proteolysis. *Trends in Plant Science*, *7*, 451–456.

Almeida, J., Quadrana, L., Asís, R., Setta, N., de Godoy, F., Bermúdez, L., … Rossi, M. (2011). Genetic dissection of vitamin E biosynthesis in tomato. *Journal of Experimental Botany*, *62*, 3781–3798.

Alseekh, S., Ofner, I., Pleban, T., Tripodi, P., Di Dato, F., Cammareri, M., … Zamir, D. (2013). Resolution by recombination: Breaking up *Solanum pennellii* introgressions. *Trends in Plant Science*, *18*, 536–538.

Araújo, W. L., Nunes-Nesi, A., Osorio, S., Usadel, B., Fuentes, D., Nagy, R., … Fernie, A. R. (2011). Antisense inhibition of the iron-sulphur subunit of succinate dehydrogenase enhances photosynthesis and growth in tomato via an organic acid-mediated effect on stomatal aperture. *Plant Cell*, *23*, 600–627.

Aucique-Perez, C. E., Rodrigues, F. A., Moreira, W. R., & DaMatta, F. M. (2014). Leaf gas exchange and chlorophyll a fluorescence in wheat plants supplied with silicon and infected with *Pyricularia oryzae*. *Phytopathology*, *104*, 143–149.

Baker, N. R., & Rosenqvist, E. (2004). Applications of chlorophyll fluorescence can improve crop production strategies: An examination of future possibilities. *Journal of Experimental Botany*, *55*, 1607–1621.

Baxter, C. J., Carrari, F., Bauke, A., Overy, S., Hill, S. A., Quick, P. W., … Sweetlove, L. J. (2005). Fruit carbohydrate metabolism in an introgression line of tomato with increased fruit soluble solids. *Plant and Cell Physiology*, *46*, 425–437.

Benjamini, Y., & Hochberg, Y. (1995). Controlling the false discovery rate: A practical and powerful approach to multiple testing. *Journal of the Royal Statistical Society B*, *57*, 289–300.

Bertin, P., & Gallais, A. (2001). Genetic variation for nitrogen use efficiency in a set of recombinant inbred lines II - QTL detection and coincidences. *Maydica*, *46*, 53–68.

Bolger, A., Scossa, F., Bolger, M. E., Lanz, C., Maumus, F., Tohge, T., … Fernie, A. R. (2014). The genome of the stress-tolerant wild tomato species *Solanum pennellii*. *Nature Genetics*, *46*, 1034–1038.

Braun, H., Binder, S., Brennicke, A., Eubel, H., Fernie, A. R., Finkemeier, I., … Zehrmann, A. (2014). The life of plant mitochondrial complex I. *Mitochondrion*, *19*, 295–313.

Cairns, J. R. K., & Esen, A. (2010). β-Glucosidases. *Cellular and Molecular Life Sciences*, *67*, 3389–3405.

Caldana, C., Scheible, W. R., Mueller-Roeber, B., & Ruzicic, S. (2007). A quantitative RT-PCR platform for high-throughput expression profiling of 2500 rice transcription factors. *Plant Methods*, *3*, 7.

Carrari, F., Nunes-Nesi, A., Gibon, Y., Lytovchenko, A., Loureiro, M. E., & Fernie, A. R. (2003). Reduced expression of aconitase results in an enhanced rate of photosynthesis and marked shifts in carbon partitioning in illuminated leaves of wild species tomato. *Plant Physiology*, *133*, 1322–1335.

Causse, M., Duffe, P., Gomez, M. C., Buret, M., Damidaux, R., Zamir, D., … Rothan, C. (2004). A genetic map of candidate genes and QTLs involved in tomato fruit size and composition. *Journal of Experimental Botany*, *55*, 1671–1685.

Chitwood, D. H., Kumar, R., Headland, L. R., Ranjan, A., Covington, M. F., Ichihashi, Y., … Sinha, N. R. (2013). A quantitative genetic basis for leaf morphology in a set of precisely defined tomato introgression lines. *The Plant Cell*, *25*, 2465–2248.

Condon, A. G., Richards, R. A., Rebetzke, G. J., & Farqhuar, G. D. (2004). Breeding for high water use efficiency. *Journal of Experimental Botany*, *55*, 2447–2460.

Conesa, A., Götz, S., García-Gómez, J. M., Terol, J., Talón, M., & Robles, M. (2005). Blast2GO: A universal tool for annotation, visualization and analysis in functional genomics research. *Bioinformatics*, *21*, 3674–3676.

Cross, J. M., von Korff, M., Altmann, T., Bartzetko, L., Sulpice, R., Gibon, Y., … Stitt, M. (2006). Variation of enzyme activities and metabolite levels in 24 *Arabidopsis* accessions growing in carbon-limited conditions. *Plant Physiology*, *142*, 1574–1588.

Cruz, C. D. (2013). GENES - a software package for analysis in experimental statistics and quantitative genetics. *Acta Scientiarum Agronomy*, *35*, 271–276.

de Godoy, F., Bermudez, L., Lira, B. S., de Souza, A. P., Elbl, P., Demarco, D., … Rossi, M. (2013). Galacturonosyltransferase 4 silencing alters pectin composition and carbon partitioning in tomato. *Journal of Experimental Botany*, *64*, 2449–2466.

Demura, T., & Zheng-Hua, Y. (2010). Regulation of plant biomass production. *Current Opinion in Plant Biology*, *13*, 298–303.

Do, P. T., Prudent, M., Sulpice, R., Causse, M., & Fernie, A. R. (2010). The influence of fruit load on the tomato pericarp metabolome in a *Solanum chmielewskii* introgression line population. *Plant Physiology*, *154*, 1128–1142.

Driever, S. M., Lawson, T., Andralojc, P. J., Raines, C. A., & Parry, M. A. (2014). Natural variation in photosynthetic capacity, growth, and yield in 64 field-grown wheat genotypes. *Journal of Experimental Botany*, *65*, 1–15.

Eisenhut, M., Hocken, N., & Weber, A. P. M. (2015). Plastidial metabolite transporters integrate photorespiration with carbon, nitrogen, and sulfur metabolism. *Cell Calcium*, *58*, 98–104.

El-Lithy, M. E., Rodrigues, G. C., van Rensen, J. J., Snel, J. F., Dassen, H. J., Koornneef, M., … Vreugdenhil, D. (2005). Altered photosynthetic performance of a natural *Arabidopsis* accession is associated with atrazine resistance. *Journal of Experimental Botany*, *56*, 1625–1634.

Eshed, Y., & Zamir, D. (1995). An introgression line population. *Genetics*, *141*, 1147–1162.

Fanourakis, D., Giday, H., Milla, R., Pieruschka, R., Kjaer, K. H., Bolger, M., … Ottosen, C. O. (2015). Pore size regulates operating stomatal conductance, while stomatal densities drive the partitioning of conductance between leaf sides. *Annals of Botany*, *115*, 555–565.

Fernie, A. R., Roscher, A., Ratcliffe, R. G., & Kruger, N. J. (2001). Fructose 2,6-bisphosphate activates pyrophosphate: Fructose-6-phosphate 1-phosphotransferase and increases triose phosphate to hexose phosphate cycling heterotrophic cells. *Planta*, *212*, 250–263.

Flood, P. J., Harbinson, J., & Aarts, M. G. (2011). Natural genetic variation in plant photosynthesis. *Trends in Plant Science*, *16*, 327–335.

Frary, A., Nesbitt, T. C., Grandillo, S., Knaap, E., Cong, B., Liu, J., … Tanksley, S. D. (2000). Fw2.2: A quantitative trait locus key to the evolution of tomato fruit size. *Science*, *289*, 85–88.

Frei, M., Tanaka, J. P., & Wissuwa, M. (2008). Genotypic variation in tolerance to elevated ozone in rice: Dissection of distinct genetic factors linked to tolerance mechanisms. *Journal of Experimental Botany*, *59*, 3741–3752.

Fridman, E., Carrari, F., Liu, Y. S., Fernie, A. R., & Zamir, D. (2004). Zooming in on a quantitative trait for tomato yield using interspecific introgressions. *Science*, *305*, 1786–1789.

Fridman, E., Pleban, T., & Zamir, D. (2000). A recombination hotspot delimits a wild-species quantitative trait locus for tomato sugar content to 484 bp within an invertase gene. *Proceedings of the National Academy of Sciences of the United States of America*, *97*, 4718–4723.

Gago, J., de Menezes Daloso, D., Figueroa, C. M., Flexas, J., Fernie, A. R., & Nikoloski, Z. (2016). Relationships of leaf net photosynthesis, stomatal conductance, and mesophyll conductance to primary metabolism: A multispecies meta-analysis approach. *Plant Physiology*, *171*, 265–279.

Geisler, D. A., Papke, C., Obata, T., Nunes-Nesi, A., Matthes, A., Schneitz, K., … Persson, S. (2012). Downregulation of the δ-subunit reduces mitochondrial ATP synthase levels, alters respiration, and restricts growth and gametophyte development in *Arabidopsis*. *Plant Cell*, *24*, 2792–2811.

Grodzinski, B., Jiao, J., Knowles, V. L., & Plaxton, W. C. (1999). Photosynthesis and carbon partitioning in transgenic tobacco plants deficient in leaf cytosolic pyruvate kinase. *Plant Physiology*, *120*, 887–896.

Gu, J., Yin, X., Struik, P. C., Stomph, T. J., & Wang, H. (2012). Using chromosome introgression lines to map quantitative trait loci for photosynthesis parameters in rice (*Oryza sativa* L.) leaves under drought and well-watered field conditions. *Journal of Experimental Botany*, *63*, 455–469.

Hackel, A., Schauer, N., Carrari, F., Fernie, A. R., Grimm, B., & Kühn, C. (2006). Sucrose transporter LeSUT1 and LeSUT2 inhibition affects tomato fruit development in different ways. *The Plant Journal*, *45*, 180–192.

Hajirezaei, M., Sonnewald, U., Viola, R., Carlisle, S., Dennis, D., & Stitt, M. (1994). Transgenic potato plants with strongly decreased expression of pyrophosphate:Fructose-6-phosphate phosphotransferase show no visible phenotype and only minor changes in metabolic fluxes in their tubers. *Planta*, *192*, 16–30.

Hikosaka, K. (2010). Mechanisms underlying interspecific variation in photosynthetic capacity across wild plant species. *Plant Biotechnology*, *27*, 223–229.

Holtan, H. E., & Hake, S. (2003). Quantitative trait locus analysis of leaf dissection in tomato using *Lycopersicon pennellii* segmental introgression lines. *Genetics*, *165*, 1541–1550.

Hunt, R. (1982). *Plant growth curves: The functional approach to plant growth analysis*(pp. 248). London: Edward Arnold.

Jackson, P., Basnayake, J., Inman-Bamber, G., Lakshmanan, P., Natarajan, S., & Stokes, C. (2016). Genetic variation in transpiration efficiency and relationships between whole plant and leaf gas exchange measurements in *Saccharum* spp. and related germplasm. *Journal of Experimental Botany*, *67*, 861–871.

Kamenetzky, L., Asís, R., Bassi, S., de Godoy, F., Bermúdez, L., Fernie, A. R., … Carrari, F. (2010). Genomic analysis of wild tomato introgressions determining metabolism- and yield-associated traits. *Plant Physiology*, *152*, 1772–1786.

Kangasjärvi, S., Neukermans, J., Li, S., Aro, E. M., & Noctor, G. (2012). Photosynthesis, photorespiration, and light signalling in defence responses. *Journal of Experimental Botany*, *63*, 1619–1636.

Khowaja, F. S., & Price, A. H. (2008). QTL mapping rolling, stomatal conductance and dimension traits of excised leaves in the Bala *x* Azucena recombinant inbred population of rice. *Field Crops Research*, *106*, 248–257.

Knowles, V. L., Mchugh, S. G., Hu, Z., Dennis, D. T., Miki, B. L., & Plaxton, W. C. (1998). Altered growth of transgenic tobacco lacking leaf cytosolic pyruvate kinase. *Plant Physiology*, *116*, 45–51.

Koornneef, M., Alonso-Blanco, C., & Vreugdenhil, D. (2004). Naturally occurring genetic variation in *Arabidopsis thaliana*. *Annual Review of Plant Biology*, *55*, 141–172.

Lawson, T., Kramer, D. M., & Raines, C. A. (2012). Improving yield by exploiting mechanisms underlying natural variation of photosynthesis. *Current Opinion in Biotechnology*, *23*, 215–220.

Li, H., Tong, Y., Li, B., Jing, R., Lu, C., & Li, Z. (2010). Genetic analysis of tolerance to photo-oxidative stress induced by high light in winter wheat (*Triticum aestivum* L.). *Journal of Genetics and Genomics*, *37*, 399–412.

Liang, Y., Zhang, K., Zhao, L., Liu, B., Meng, Q., & Tian, J. (2010). Identification of chromosome regions conferring dry matter accumulation and photosynthesis in wheat (*Triticum aestivum* L.). *Euphytica*, *171*, 145–156.

Lipka, V., Dittgen, J., Bednarek, P., Bhat, R., Wiermer, M., Stein, M., … Schulze-Lefert, P. (2005). Pre- and postinvasion defenses both contribute to nonhost resistance in *Arabidopsis*. *Science*, *310*, 1180–1183.

Liu, Y., Gur, A., Ronen, G., Causse, M., Damidaux, R., Buret, M., … Zamir, D. (2003). There is more to tomato fruit colour than candidate carotenoid genes. *Plant Biotechnology Journal*, *1*, 195–207.

Lytovchenko, A., Eickmeier, I., Pons, C., Osorio, S., Szecowka, M., Lehmberg, K., … Fernie, A. R. (2011). Tomato fruit photosynthesis is seemingly unimportant in primary metabolism and ripening but plays a considerable role in seed development. *Plant Physiology*, *157*, 1650–1663.

Malboobi, M. A., & Lefebvre, D. D. (1997). A phosphate-starvation inducible β-glucosidase gene (psr3.2) isolated from *Arabidopsis thaliana* is a member of a distinct subfamily of the BGA family. *Plant Molecular Biology*, *34*, 57–68.

Medeiros, D. B., Martins, S. C., Cavalcanti, J. H., Daloso, D. M., Martinoia, E., Nunes-Nesi, A., … Araújo, W. L. (2015). Enhanced photosynthesis and growth in atquac1 knockout mutants are due to altered organic acid accumulation and an increase in both stomatal and mesophyll conductance. *Plant Physiology*, *170*, 86–101.

Mertens, E., Larondelle, Y., & Hers, H. (1990). Induction of pyrophosphate: Fructose 6-phosphate 1-phosphotransferase by anoxia in rice seedlings. *Plant Physiology*, *93*, 584–587.

Meyer, E. H., Tomaz, T., Carroll, A. J., Estavillo, G., Delannoy, E., Tanz, S. K., … National, A. (2009). Remodeled respiration in ndufs4 with low phosphorylation efficiency suppresses Arabidopsis germination and growth and alters control of metabolism at night. *Plant Physiology*, *151*, 603–619.

Meyer, R. C., Steinfath, M., Lisec, J., Becher, M., Witucka-Wall, H., Törjék, O., … Altmann, T. (2007). The metabolic signature related to high plant growth rate in *Arabidopsis thaliana*. *Proceedings of the National Academy of Sciences of the United States of America*, *104*, 4759–4764.

Mozdzer, T. J., & Zieman, J. C. (2010). Ecophysiological differences between genetic lineages facilitate the invasion of non-native *Phragmites australis* in north American Atlantic coast wetlands. *Journal of Ecology*, *98*, 451–458.

Muir, C. D., Hangarter, R. P., Moyle, L. C., & Davis, P. A. (2014). Morphological and anatomical determinants of mesophyll conductance in wild relatives of tomato (*Solanum* sect. *Lycopersicon*, sect. *Lycopersicoides*; *Solanaceae*). *Plant*. *Cell and Environment*, *37*, 1415–1426.

Muir, C. D., Pease, J. B., & Moyle, L. C. (2014). Quantitative genetic analysis indicates natural selection on leaf phenotypes across wild tomato species (*Solanum* sect. *Lycopersicon*; *Solanaceae*). *Genetics*, *198*, 1629–1643.

Murashige, T., & Skoog, F. (1962). A revised medium for rapid growth and bio assays with tobacco tissue cultures. *Physiologia Plantarum*, *15*, 473–497.

Mustroph, A., Sonnewald, U., & Biemelt, S. (2007). Characterisation of the ATP-dependent phosphofructokinase gene family from *Arabidopsis thaliana*. *FEBS Letters*, *581*, 2401–2410.

Noctor, G., Dutilleul, C., De Paepe, R., & Foyer, C. H. (2004). Use of mitochondrial electron transport mutants to evaluate the effects of redox state on photosynthesis, stress tolerance and the integration of carbon/nitrogen metabolism. *Journal of Experimental Botany*, *55*, 49–57.

Norby, R., Wullschleger, S., Hanson, P., Gundeson, C., Tschaplinski, T., & Jastrow, J. (2006). In J. Nosberger, S. Long, R. Norby, M. Stitt, G. Hendrey, & H. Blum (Eds.), *Managed ecosystems and CO2 case studies, processes, and perspectives* (pp. 231–251). Berlin Heidelberg: Ecol. Stud. Springer-Verlag Berlin Heidelberg.

Nunes-Nesi, A., Carrari, F., Gibon, Y., Sulpice, R., Lytovchenko, A., Fisahn, J., … Fernie, A. R. (2007). Deficiency of mitochondrial fumarase activity in tomato plants impairs photosynthesis via an effect on stomatal function. *The Plant Journal*, *50*, 1093–1106.

Nunes-Nesi, A., Carrari, F., Lytovchenko, A., Smith, A. M., Loureiro, M. E., Ratcliffe, R. G., … Fernie, A. R. (2005). Enhanced photosynthetic performance and growth as a consequence of decreasing mitochondrial malate dehydrogenase activity in transgenic tomato plants. *Plant Physiology*, *137*, 611–622.

Ort, D. R., Merchant, S. S., Alric, J., Barkan, A., Blankenship, R. E., Bock, R., … Zhu, X. G. (2015). Redesigning photosynthesis to sustainably meet global food and bioenergy demand. *Proceedings of the National Academy of Sciences of the United States of America*, *112*, 8529–8536.

Oyanedel, E., Wolfe, D. W., Owens, T. G., Monforte, A. J., & Tanksley, S. D. (2000). Quantitative trait loci analysis of photoinhibition under chilling stress in tomato. *Acta Horticulturae*, *52*, 227–232.

Price, A. H., Young, E. M., & Tomos, A. D. (1997). Quantitative trait loci associated with stomatal conductance, leaf rolling and heading date mapped in upland rice (*Oryza sativa*). *New Phytologist*, *137*, 83–91.

Quadrana, L., Almeida, J., Asís, R., Duffy, T., Dominguez, P. G., Bermúdez, L., … Carrari, F. (2014). Natural occurring epialleles determine vitamin E accumulation in tomato fruits. *Nature Communications*, *5*, 3027.

Riebeseel, E., Häusler, R. E., Radchuk, R., Meitzel, T., Hajirezaei, M. R., Emery, R. J., … Weber, H. (2010). The 2-oxoglutarate/malate translocator mediates amino acid and storage protein biosynthesis in pea embryos. *The Plant Journal*, *61*, 350–363.

Ron, M., Dorrity, M. W.,de Lucas, M., Toal, T., Hernandez, R. I., Little, S. A., … Brady, S. M. (2013). Identification of novel loci regulating interspecific variation in root morphology and cellular development in tomato. *Plant Physiology*, *162*, 755–768.

Ronen, G., Carmel-Goren, L., Zamir, D., & Hirschberg, J. (2000). An alternative pathway to beta-carotene formation in plant chromoplasts discovered by map-based cloning of beta and old-gold color mutations in tomato. *Proceedings of the National Academy of Sciences of the United States of America*, *97*, 11102–11107.

Rosado-Souza, L., Scossa, F., Chaves, I. S., Kleessen, S., Salvador, L. F. D., Milagre, J. C., … Nunes-Nesi, A. (2015). Exploring natural variation of photosynthetic, primary metabolism and growth parameters in a large panel of *Capsicum chinense* accessions. *Planta*, *242*, 677–691.

Rossi, M., Bermudez, L., & Carrari, F. (2015). Crop yield: Challenges from a metabolic perspective. *Current Opinion in Plant Biology*, *25*, 79–89.

Schauer N, Semel Y, Roessner U, Gur A, Balbo I, Carrari F., …, Fernie A.R. (2006) Comprehensive metabolic profiling and phenotyping of interspecific introgression lines for tomato improvement. *Nature Biotechnology 24*, 447–454.

Schauer, N., Zamir, D., & Fernie, A. R. (2005). Metabolic profiling of leaves and fruit of wild species tomato: A survey of the *Solanum lycopersicum* complex. *Journal of Experimental Botany*, *56*, 297–307.

Schilmiller, A., Shi, F., Kim, J., Charbonneau, A. L., Holmes, D., Daniel, J. A., & Last, R. L. (2010). Mass spectrometry screening reveals widespread diversity in trichome specialized metabolites of tomato chromosomal substitution lines. *The Plant Journal*, *62*, 391–403.

Schneidereit, J., Häusler, R. E., Fiene, G., Kaiser, W. M., & Weber, A. P. (2006). Antisense repression reveals a crucial role of the plastidic 2-oxoglutarate/malate translocator DiT1 at the interface between carbon and nitrogen metabolism. *The Plant Journal*, *45*, 206–224.

Schreiber, U., Hormann, H., Neubauer, C., & Klughammer, C. (1995). Assessment of photosystem II photochemical quantum yield by chlorophyll fluorescence quenching analysis. *Functional Plant Biology*, *22*, 209–220.

Semel, Y., Nissenbaum, J., Menda, N., Zinder, M., Krieger, U., Issman, N., … Zamir, D. (2006). Overdominant quantitative trait loci for yield and fitness in tomato. *Proceedings of the National Academy of Sciences of the United States of America*, *103*, 12981–12986.

Simkin, A., McAusland, L., Headland, L., Lawson, T., & Raines, C. (2015). Multigene manipulation of photosynthetic carbon assimilation increases CO_2 fixation and biomass yield in tobacco. *Journal of Experimental Botany*, *66*, 4075–4090.

Sjögren, L. L., Stanne, T. M., Zheng, B., Sutinen, S., & Clarke, A. K. (2006). Structural and functional insights into the chloroplast ATP-dependent Clp protease in Arabidopsis. *Plant Cell*, *18*, 2635–2649.

Stanke, M., Steinkamp, R., Waack, S., & Morgenstern, B. (2004). AUGUSTUS: A web server for gene finding in eukaryotes. *Nucleic Acids Research*, *32*, W309–W312.

Steinhauser, M. C., Steinhauser, D., Gibon, Y., Bolger, M., Arrivault, S., Usadel, B., … Stitt, M. (2011). Identification of enzyme activity quantitative trait loci in a *Solanum lycopersicum* x *Solanum pennellii* introgression line population. *Plant Physiology*, *157*, 998–1014.

Sulpice, R., Pyl, E. T., Ishihara, H., Trenkamp, S., Steinfath, M., Witucka-Wall, H., … Stitt, M. (2009). Starch as a major integrator in the regulation of plant growth. *Proceedings of the National Academy of Sciences of the United States of America*, *106*, 10348–10353.

Takahashi, S., Bauwe, H., & Badger, M. (2007). Impairment of the photorespiratory pathway accelerates photoinhibition of photosystem II by suppression of repair but not acceleration of damage processes in Arabidopsis. *Plant Physiology*, *144*, 487–494.

Tieman, D. M., Zeigler, M., Schmelz, E. A., Taylor, M. G., Bliss, P., Kirst, M., & Klee, H. J. (2006). Identification of loci affecting flavour volatile emissions in tomato fruits. *Journal of Experimental Botany*, *57*, 887–896.

Valentini, R., Epron, D., Angelis, P., Matteucci, G., & Dreyer, E. (1995). In situ estimation of net CO_2 assimilation, photosynthetic electron flow and photorespiration in Turkey oak (*Q. cerris* L.) leaves: Diurnal cycles under different levels of water supply. *Plant, Cell and Environment*, *18*, 631–640.

van Rooijen, R., Aarts, M. G., & Harbinson, J. (2015). Natural genetic variation for acclimation of photosynthetic light use efficiency to growth irradiance in *Arabidopsis thaliana*. *Plant Physiology*, *167*, 1412–1429.

Wen, W., Liu, H., Zhou, Y., Jin, M., Yang, N., Li, D., … Fernie, A. R. (2016). Combining quantitative genetics approaches with regulatory network analysis to dissect the complex metabolism of the maize kernel. *Plant Physiology*, *170*, 136–146.

Xu, X., Martin, B., Comstock, J. P., Vision, T. J., Tauer, C. G., Zhao, B., … Knapp, S. (2008). Fine mapping a QTL for carbon isotope composition in tomato. *Theoretical and Applied Genetics*, *117*, 221–233.

Yang, D. L., Jing, R. L., Chang, X. P., & Li, W. (2007). Quantitative trait loci mapping for chlorophyll fluorescence and associated traits in wheat (*Triticum aestivum*). *Journal of Integrative Plant Biology*, *49*, 646–654.

Yin, Z., Meng, F., Song, H., He, X., Xu, X., & Yu, D. (2010). Mapping quantitative trait loci associated with chlorophyll a fluorescence parameters in soybean (*Glycine max* (L.) Merr.). *Planta*, *231*, 875–885.

Zhang, K., Fang, Z., Liang, Y., & Tian, J. (2009). Genetic dissection of chlorophyll content at different growth stages in common wheat. *Journal of Genetics*, *88*, 183–189.

Zhang, N., Gibon, Y., Jason, G. W., Nick, K. L., Li, P., Dedow, L., … Thomas, P. B. (2015). Genome-wide association of carbon and nitrogen metabolism in the maize nested association mapping population. *Plant Physiology*, *168*, 575–583.

Zou, J., Rogers, W., & Siemann, E. (2007). Differences in morphological and physiological traits between native and invasive populations of *Sapium sebiferum*. *Functional Ecology*, *21*, 721–730.

SUPPORTING INFORMATION

Additional Supporting Information may be found online in the supporting information tab for this article.

How to cite this article: de Oliveira Silva FM, Lichtenstein G, Alseekh S, et al. The genetic architecture of photosynthesis and plant growth-related traits in tomato. *Plant Cell Environ*. 2018;41:327–341. https://doi.org/10.1111/pce.13084